

Observational Support for Massive Black Hole Formation Driven by Runaway Stellar Collisions in Galactic Nuclei.

Andrés Escala

Departamento de Astronomía, Universidad de Chile, Casilla 36-D, Santiago, Chile.

aescala@das.uchile.cl

ABSTRACT

We explore here an scenario for massive black hole formation driven by stellar collisions in galactic nuclei, proposing a new formation regime of global instability in nuclear stellar clusters triggered by runaway stellar collisions. Using order of magnitude estimations, we show that observed nuclear stellar clusters avoid the regime where stellar collisions are dynamically relevant over the whole system, while resolved detections of massive black holes are well into such collision-dominated regime. We interpret this result in terms of massive black holes and nuclear stellar clusters being different evolutionary paths of a common formation mechanism, unified under the standard terminology of being both central massive objects. We propose a formation scenario where central massive objects more massive than $\sim 10^8 M_\odot$, which also have relaxation times longer than their collision times, will be too dense (in virial equilibrium) to be globally stable against stellar collisions and most of its mass will collapse towards the formation of a massive black hole. Contrarily, this will only be the case at the core of less dense central massive objects leading to the formation of black holes with much lower black hole efficiencies $\epsilon_{\text{BH}} = \frac{M_{\text{BH}}}{M_{\text{CMO}}}$, with these efficiencies ϵ_{BH} drastically growing for central massive objects more massive than $\sim 10^7 M_\odot$, approaching unity around $M_{\text{CMO}} \sim 10^8 M_\odot$. We show that the proposed scenario successfully explains the relative trends observed in the masses, efficiencies, and scaling relations between massive black holes and nuclear stellar clusters.

1. Introduction

For more than half a century, evidence was accumulated for the existence of Massive Black Holes (MBHs) in galactic nuclei with masses $\sim 10^{6-9} M_\odot$ (Zel'dovich 1964; Salpeter

1964; Ghez et al. 2008; Gillessen et al. 2009), but only recently arrived definite support in favor of their existence (The Event Horizon Telescope Collaboration 2019). The origin of such ‘monsters’ puzzled theorists soon after their discovery (Rees 1984), however, is still a mystery their dominant formation process (Volonteri 2010). With the advent of the gravitational wave astronomy, specially with the future LISA experiment (Amaro-Seoane et al. 2013; Barause et al. 2015), it is expected to have definite answers on the formation of MBHs in the universe.

Several pathways have been proposed for MBH formation (Rees 1984; Volonteri 2010; Shapiro 2004), which can be briefly summarized into 3 channels: i) Direct collapse of a primordial cloud onto a MBH (Bromm & Loeb 2003; Lodato & Natarajan 2006; Latif & Schleicher 2015; Becerra et al. 2015; Regan & Downes 2018) ii) Growth by gas accretion and/or mergers of a stellar/intermediate mass BH up to the mass range of MBHs (Madau & Rees 2001; Volonteri et al. 2003; Agarwal et al. 2013; Ricarte & Natarajan 2018) and iii) Formation of a MBH by catastrophic stellar collisions in dense stellar clusters (Zel’dovich & Podurets 1965; Rees 1984; Shapiro & Teukolsky 1985; Omukai et al. 2008; Devecchi & Volonteri 2009; Devecchi et al. 2014). However, all of them faced severe problems to fulfill the constraints set by observations, such as the physical conditions needed to sustain atomic cooling halos are unclear to be fulfilled (i; Shang et al. 2010; Inayoshi & Haiman 2014; Suazo et al. 2019), problems for explaining the highest redshift quasars by lower mass BHs grown thru Eddington-limited accretion (ii; Gnedin 2001; Volonteri & Rees 2006; Prieto et al. 2017; Inayoshi et al. 2020) and that simulations of stellar collisions in dense clusters are able to form only BHs of lower masses in the intermediate mass regime (iii; Portegies Zwart & McMillan 2002; Freitag et al. 2006a,b; Goswami et al. 2012; Stone et al. 2017).

Besides the problems faced by the different formation scenarios, galactic centers are arguably the most favorable places for MBH formation. Any gaseous (and stellar) material that eventually loses its orbital support falls on to this preferential place (Shlosman et al. 1990; Escala 2006), which corresponds to the deepest part of the galactic gravitational potential. Multiple processes produces strong inflows at galactic scales on dynamical timescales, funneling large amount of gaseous material (up to $10^{10} M_{\odot}$) to this preferential place, that includes gravitational torques in galaxy mergers (Barnes 2002; Mayer et al 2010; Prieto et al 2020), bars within bars (Regan & Teuben 2004; Hopkins & Quataert 2010), clump migration by dynamical friction (Escala 2007; Elmegreen et al. 2008), etc. These processes are expected to be even more dramatic in the case of proto-galactic material at high z , because of the higher gas fractions and the absence of AGN feedback from preexisting MBHs (Prieto & Escala 2016). Therefore, in the absence of feedback limiting factors (Dubois et al. 2015; Prieto et al. 2017), the amount of material funneled into galactic nuclei has (in principle) no upper limit externally set by processes at galactic scales and thus, we expect to be the hosting place of the densest gaseous and stellar configurations in the universe. The straightforward

question is then, if such material it does not ends up forming a MBH, that corresponds to gravity’s final triumph, which other stable physical configuration (at intermediate densities) it could be?

The hypothetical scenario under very efficient heating mechanisms ($T_{\text{vir}} \geq 10^4\text{K}$) has been extensively studied (Bromm & Loeb 2003; Lodato & Natarajan 2006; Latif & Schleicher 2015; Becerra et al. 2015; Regan & Downes 2018), where fragmentation is suppressed on smaller scales and that directly leads to the formation of a single Very Massive quasi-Star (VMS; Volonteri & Begelman 2010; Schleicher et al. 2013) at the center, which afterwards collapses onto a MBH due to post-Newtonian instability (Tolman 1934; Oppenheimer & Volkoff 1939). Contrarily, in the absence of efficient heating the gaseous material funneled to the galactic center efficiently cools (Rees & Ostriker 1977; Sarazin & White 1987), eventually becomes unstable and fragments in a broad range of scales (Toomre 1964; Escala & Larson 2008; Escala 2011), leading to the formation of a dense stellar cluster (Bate et al. 2003; Padoan et al. 2016). Such dense stellar configurations are indeed observed, being called Nuclear Stellar Clusters (NSCs) and that are considered the densest stellar configurations in the local Universe (Boker et al. 2004; Cote et al. 2006; Walcher et al. 2006; Balcells et al. 2007), located in galactic nuclei and where in some cases coexists with a MBH (Leigh et al. 2012; Georgiev et al 2016), thus having possibly a joint formation event. Therefore, a more realistic scenario reduces to how dense such stellar system it can be before becoming globally unstable, leading it again to the formation of a MBH.

A natural candidate for triggering instability in stellar clusters are collisions between stars since it is an efficient mechanism for losing orbital energy support, because physical collisions between stars are a dissipative source on a fluid interpretation of a cluster, being able to convert energy in kinetic motions into internal heat of stars and that otherwise, without collisions the energy in stellar motions behaves adiabatically. However, it is generally believed that physical collisions between stars are considered an exotic phenomena that rarely happen in the universe (Binney & Tremaine 2008), restricted to only be relevant in the cores of dense stellar configurations like Globular Clusters systems (Portegies Zwart et al. 1999), where it is well established that the cores of such dense stellar systems are unstable to suffer catastrophic runaway stellar collisions (Portegies Zwart & McMillan 2002). Numerical experiments have shown that runaway collisions of the most massive stars could led to the formation of Intermediate-Mass Black Holes (IMBHs) in the centers of typical globular clusters (BH masses $\sim 10^3 M_{\odot}$ can be build up before the first supernova explodes; Portegies Zwart & McMillan 2002; Freitag et al. 2006a,b; Gurkan et al. 2004). Nevertheless, it is unclear what could happen in the more extreme conditions of proto-galactic nucleus, because of the lack of detailed N-body simulations that includes the effects of the higher densities and velocity dispersions, that in addition to gas dissipation should define a density limit for

NSCs before becoming globally unstable to catastrophic stellar collisions.

In this paper, we will study the role of runaway stellar collisions in galactic nuclei, particularly, in the global stability of NSCs and the possible formation of MBHs. We start quantifying the role of collisions in NSCs in §2. We continue in §3 proposing an scenario for MBH formation in galactic nuclei from NSCs. Finally, we discuss the results of the proposed scenario and its implications for the high redshift universe in §4.

2. Quantifying the Role of Collisions in Nuclear Stellar Clusters

An order of magnitude estimate that quantifies the occurrence of collisions in any system with large number of particles, is to compute a collision timescale given by $t_{\text{coll}} = \lambda/\sigma$, where σ is the characteristic (dispersion) velocity of the system and λ is the particle (star) mean free path (Binney & Tremaine 2008). From the equation $n\Sigma_o\lambda = 1$ a mean free path can be probabilistically defined (Landau & Lifshitz 1980; Shu 1991), where n is the number density of stars and Σ_o the effective cross section, giving a collision rate of $t_{\text{coll}}^{-1} = n\Sigma_o\sigma$. This is a widely used definition for collision timescale, accurate enough for the general purpose of this paper, for a more specific formula that could be better to quantify collision rates in a particular problem see for example Leigh et al (2014). Assuming that the stellar system is virialized, the dispersion velocity is $\sigma = (GM/R)^{1/2}$, where M is the total mass and R the characteristic radius of the system. This result is generally valid in any stellar system in virial equilibrium and is also valid for systems with a relevant dark matter component, using the empirically calibrated formula of (Cappellari et al., 2006), where the velocity dispersion is $\sigma = (GM/5f_gR)^{1/2} \approx (GM/R)^{1/2}$ for $f_g = 0.16$ (Spergel et al., 2003). Therefore, in any virialized stellar system the collision timescale is given by

$$t_{\text{coll}} = \frac{1}{n\Sigma_o} \sqrt{\frac{R}{GM}} \quad . \quad (1)$$

In an uniform system, composed only by solar mass stars, the number density is $n = 3M/4\pi R^3 M_\odot$. The effective cross section Σ_o , due to gravitational focusing, is for a solar mass star approximately $100 \pi R_\odot^2$ (i.e. Eq 7.195 in Binney & Tremaine 2008, with a Safronov number for solar mass stars with a $\sigma \sim 100 \text{km s}^{-1}$; Leigh et al. 2012). Under these assumptions, neglecting radial concentrations, initial mass functions and other dimensionless factors of order unity, collisions will be relevant in the dynamics (and possibly becoming unstable) of a given system with a characteristic age t_H , if its age is comparable or longer

than the collision time, $t_{\text{coll}} \leq t_{\text{H}}$, which is equivalent to the following condition:

$$\hat{\rho}_{\text{crit}} \equiv \left(\frac{4M_{\odot}}{300R_{\odot}^2 t_{\text{H}} G^{1/2}} \right)^{2/3} \leq MR^{-\frac{7}{3}}, \quad (2)$$

where $\hat{\rho}_{\text{crit}}$ is a critical mass density, an intermediate density between the surface density ($\propto R^{-2}$) and a volumetric one ($\propto R^{-3}$). The largest relevant value for t_{H} is the age of the universe, which is of the order of $\sim 10^{10}$ years (Spergel et al., 2003) that gives a (minimal) critical mass density $\hat{\rho}_{\text{crit}} \sim 10^7 M_{\odot} \text{pc}^{-7/3}$, but galactic centers can be one order of magnitude younger ($t_{\text{H}} \sim 10^9$ yr). Within geometrical factors of order unity, such boundary is set by a combination of a fundamental constant (G), with typical parameters of our universe such as its current age (t_{H}) and the properties of the sun (M_{\odot} , R_{\odot}), which it is considered to be an average star in the Universe, defining the critical density of stable stellar systems for our current cosmic parameters. Also, we arrive to such criterion without ad-hock assumptions, being the only assumption to be virialized, which is only a requirement for being an stationary stellar system.

Figure 1 displays the observed masses and effective radius for nuclear stellar clusters in both late- and early-type galaxies (red circles) taken from (Georgiev et al 2016). The solid blue line in Fig 1 displays the condition given by Eq. 2 for $t_{\text{H}} = 10^{10}$ years. The measured properties of NSCs (red circles) shows a clear avoidance of the regions in which collisions could be globally relevant in the internal dynamics of a cluster, with collision timescales always larger than the age of the universe (right side of the solid blue line). The only clear exception is NGC 1507, with its $\geq 10^7 M_{\odot}$ in only 0.1 pc of effective radius, however, this last measurement has estimated errors over 2000% (effective radius up to 2.3 pc that moves NGC 1507 to right side of the blue line). It is important to note that these are average collision timescales, relevant for global stability against collisions, that it can be considerably shorter at the core and therefore, these globally stable NSCs can still coexist with an unstable core which is expected to be triggered by Spitzer’s instability (Spitzer 1969; Vishniac 1978; Portegies Zwart & McMillan 2002).

In addition, we plot in Fig 1 the measured masses and resolution radius ($=0.5d_{\text{resol}}$, where d_{resol} is the observation spatial resolution) for MBH candidates, but we differentiate them between ‘well-resolved’ MBHs with influence radius R_{inf} larger than 3 spatial resolutions (black circles) and ‘unresolved’ ones ($R_{\text{inf}} < 3 d_{\text{resol}}$) with white circles, both from the sample of (Gultekin et al, 2009). Contrarily to the case of nuclear clusters, in the case of MBH candidates we see two clear trends: the properties of resolved MBHs are in the region that clearly passed to the collision-dominated regime (left side of the solid blue line) and the unresolved ones, still avoids the collision-dominated regime and coexist with the NSCs.

The trend for unresolved MBHs positions can be easily understood taking into account

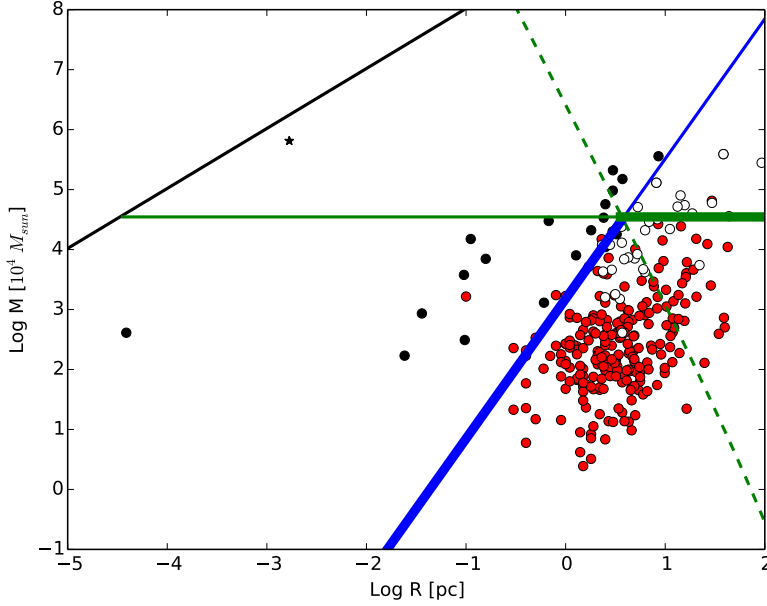


Fig. 1.— Measured masses and effective radius for nuclear stellar clusters (red circles), ‘well-resolved’ MBHs (black circles) and ‘unresolved’ MBHs (white circles). The measurement of M87’s black hole shadow (The Event Horizon Telescope Collaboration 2019) is denoted by the black star, which is the closest to the black line that represents positions of the Schwarzschild radius as a function of mass. The solid blue line represents the condition given by Eq. 2 for $t_H = 10^{10}$ years ($\hat{\rho}_{\text{crit}} \sim 10^7 M_\odot \text{pc}^{-7/3}$). The horizontal green line represents the condition implied by Eq. 3 ($\sim 3.5 \times 10^8 M_\odot$) in order to be in agreement with the observed scaling relation for NSCs (Leigh et al. 2012). The dashed green line denotes the condition given by Eq. 4 for $t_H = 10^{10}$ years, which intersects the solid blue line at the same critical mass determined by the condition given by Eq. 3. The positions of NSCs are restricted within the boundaries defined by the collisional stable region for NSCs, denoted by the thicker blue and green lines.

that the properties of MBHs are diluted due to resolution. For the unresolved MBHs, this means a decrease in densities down to values comparable to stellar densities in the nuclear regions of their host. Therefore, the unresolved MBHs can be taken as better estimates of the properties of the stellar background within R_{inf} than of MBHs itself and in some sense, they can be considered also like stellar systems. Taking this into account, the properties of NSCs clearly differs from the ones of resolved MBHs, with NSCs avoiding the collision-dominated region and resolved MBHs passing such limit, with a sharp transition from NSCs to resolved

MBHs around t_{coll} of the order of the age of the universe.

Taking also into account that for a virialized system $R = GM/\sigma^2$, the condition given by Eq. 2 can be rewritten as:

$$\sqrt{\frac{4 R_{\odot}}{300 \sigma_{\odot} t_{\text{H}}}} \leq \frac{M_{\odot}}{M} \left(\frac{\sigma}{\sigma_{\odot}} \right)^{3.5}, \quad (3)$$

with $\sigma_{\odot} = \sqrt{\frac{GM_{\odot}}{R_{\odot}}} \sim 400 \text{ km s}^{-1}$. If this condition is combined with the empirical scaling relation that constrains the properties for observed NSCs, $\frac{M_{\text{NSC}}}{10^{6.9} M_{\odot}} = \left(\frac{\sigma}{128 \text{ km/s}} \right)^{2.73} \sim \left(\frac{3\sigma}{\sigma_{\odot}} \right)^{2.73}$ (Leigh et al. 2012), gives that NSCs will be unstable for masses larger than $\sim 3.5 \times 10^8 M_{\odot}$ (for a t_{H} again of the order of the age of the universe). This condition is denoted by the horizontal green line in Fig. 1, showing again good agreement with the value of the most massive NSCs. Therefore, besides these conditions being order of magnitude estimations with simplifications, the positions of NSCs are suggestively restricted within the boundaries defined by the collisional stable region, denoted by the thicker blue and green lines in Fig. 1.

Although this trend of NSCs in Fig. 1 is very suggestive, its interpretation is nevertheless more complicated, since several additional factors needs to be taken into account. In addition to the intrinsic idealizations of these order of magnitude estimations, one very relevant factor is that Fig. 1 compares the structural properties of NSCs currently observed and not at the time of formation, which can be smaller by a factor of 10 or more in radius (Banerjee & Kroupa 2017), therefore, evolutionary processes must be taken into account. Numerical studies of the long term evolution of NSCs (and with MBHs; Baumgardt et al 2018; Pamanarev et al. 2019), have shown that their effective radius indeed expands, which implies that NSCs moved from left to right in Fig. 1 as they evolve. Such expansion is expected to happen in a self-similar manner when is only due to two-body relaxation processes ($R \propto t^{2/3}$; Henon 1965; Gieles et al. 2012;).

The two-body relaxation time is the relevant timescale for this evolution expected in the position of NSCs in Fig. 1, because it quantifies the energy exchange by two-body scattering and is generally expressed as $t_{\text{relax}} \approx \frac{0.1N}{\ln N} t_{\text{cross}}$ (Binney & Tremaine 2008), where t_{cross} is the crossing time of the cluster and N its total number of stars. For a virialized system, the crossing time is given by $t_{\text{cross}} = R/\sigma = R^{3/2}/\sqrt{GM}$ and if is composed by solar mass stars, the total number of stars is simply $N=M/M_{\odot}$. Under these assumptions, two-body relaxation will be relevant in the evolution of a system with a characteristic age t_{H} , if t_{H} is comparable or longer than the relaxation time, $t_{\text{relax}} \leq t_{\text{H}}$, which is equivalent to the

following condition:

$$R \leq \left(\frac{t_H M_\odot}{0.1} \ln(M/M_\odot) \right)^{2/3} \left(\frac{G}{M} \right)^{1/3}. \quad (4)$$

The dashed green line in Fig. 1 denotes the condition given by Eq. 4 for a characteristic cluster age comparable to age of the universe, $t_H = 10^{10}$ years, showing an intersection with the solid blue line strikingly at the same critical mass determined by the condition given by Eq. 3. NSCs that has $t_{\text{relax}} \leq t_{\text{coll}}$ (with cluster mass below the intersection), could start with a collision time shorter than the age of the universe but its effective radius will expand before collisions become important, moving its position the collisional stable region (right side of the solid blue line). On the other hand, if $t_{\text{coll}} \leq t_{\text{relax}}$ the NSCs will be not be able to expand before the onset of collisions, thus possibly becoming globally unstable against collisions. Therefore, this condition naturally explains the absence of NSC for masses larger than the intersection between the dashed green and solid blue line ($M_{\text{NSC}} \gtrsim 4 \times 10^8 M_\odot$). It is important to emphasize, that this stability condition comes from the triple equality: $t_{\text{relax}} = t_{\text{coll}} = t_H$ ($\sim 10^{10}$ yr).

Moreover, since the NSCs are clustered below the intersection between blue and dashed green lines in Fig. 1 ($t_{\text{relax}} \leq t_{\text{coll}}$), their collision times measured today can be assumed longer than it was at the formation of the NSCs, before their (effective) radius increased. Therefore, the NSCs that today displays a collision time slightly longer than the age of the universe could have had a considerably shorter collision time at formation, suggesting that those NSCs at formation crossed the condition of being in the collisional-dominated regime, $t_{\text{coll}} \leq t_H$, but was reversed since $t_{\text{relax}} \leq t_{\text{coll}}$, meaning that the initial conditions of galactic nuclei can indeed fulfill the conditions for instability, at least temporarily, and that many NSCs were at the edge of collisional instability at formation. Under different circumstances are resolved MBHs, all in the collisional-dominated regime in Fig. 1 ($t_{\text{coll}} \leq t_H$), independent to the relative value of t_{relax} , suggesting two different channels for MBH formation at least. This fact motivates us to explore a joint MBH and NSC formation scenario in the next section, in order to explain their relative trends in Fig. 1.

3. An Scenario for MBH Formation in Galactic Nuclei from Nuclear Star Clusters

Both MBHs and NSCs are observed to coexist in the nuclei of galaxies (Leigh et al. 2012; Georgiev et al 2016) suggesting to be a generic byproduct of their formation and evolution, being these two completely distinct type of objects unified into the terminology of being a Central Massive Object (CMO; Ferrarese al. 2006). MBHs dominates in galaxies with

masses larger than $10^{12}M_{\odot}$ and similarly occurs with NSCs for galaxies less massive than $10^{10}M_{\odot}$, with both coexisting in the intermediate mass regime (Georgiev et al 2016). If they are indeed different evolutionary stages of a common formation mechanism, the simplest interpretation of their different locations in Fig 1 is in terms of MBHs and NSCs being CMOs with different final fates. CMOs that are too dense to be globally stable against stellar collisions and that also fulfill the condition $t_{\text{coll}} \leq t_{\text{relax}}$, thus being unable to expand before the onset of runaway collisions, it will probably collapse towards the formation of a MBH. Contrarily, this will only be the case at best in the core of less dense clusters, being globally stable in the form of a NSC, probably coexisting on its center with a lower mass BH formed in the unstable core.

Simulations of globular-type stellar clusters ($\leq 10^6 M_{\odot}$) shows that cores are unstable to suffer catastrophic runaway stellar collisions of massive stars due to Spitzer’s instability (Portegies Zwart & McMillan 2002), as long as the cluster is enough massive and concentrated, with core collapse (relaxation) times less than those set by the evolution of their massive stars ($<3\text{-}25$ Myr). A central most massive object is generically formed with efficiencies ranging from 0.1% (Portegies Zwart & McMillan 2002; Freitag et al. 2006a,b) up to a few percentage of the cluster mass (Sakurai et al. 2018; Reinoso et al 2018), depending on multiple physical parameters such as stellar radius, (initial) stellar mass distribution, etc. The central most massive object is expected to have similar fate of a VMS, being typically out of thermal equilibrium, with Kelvin-Helmholtz timescale larger than the collision timescale (Goswami et al. 2012) and also, expected to collapse to an IMBH due to post-Newtonian instability (Tolman 1934; Oppenheimer & Volkoff 1939).

Unfortunately, direct N-body simulations do not explore either the regime of larger clusters in the NSC mass range ($> 10^6 M_{\odot}$) or the more extreme regime of globally unstable clusters ($> 10^8 M_{\odot}$), not only because its properties are more exotic but also, because they are numerically much more expensive. The few exceptions are restricted to either Monte Carlo calculations (Sanders 1970; Gurkan et al. 2004) or self-consistent Fokker-Planck models of galactic nuclei (Lee 1987; Quinlan & Shapiro 1990) but their results are already quite suggestive, finding that in large N systems ($> 10^7$ stars; which corresponds to cluster masses larger than $10^7 M_{\odot}$, assuming solar mass stars) three-body binary heating is unable to reverse core collapse before the onset of runaway collisions and then are vulnerable to a ‘merger instability’, which may lead to the formation of a central black hole (Lee 1987; Quinlan & Shapiro 1990). Since in this regime the collision runaway started well before core collapse and for a system with (initially) equal mass stars (Lee 1987; Quinlan & Shapiro 1990), without even requiring Spitzer’s instability, it is reasonable to expect in those systems efficiencies $M_{\text{BH}}/M_{\text{cluster}}$ higher than the few percentage found in N-body simulations of globular-type stellar clusters. NSCs are indeed expected to be the most favorable places for stellar collisions

in the Universe.

More recently, Davies, Miller & Bellovary (2011); Miller and Davies (2012) extended the work of Quinlan & Shapiro (1990) using analytical estimations to determine the stability of NSCs against stellar collisions. In particular, Miller and Davies (2012) studied different paths for MBH formation in NSCs and determined, that MBHs should form in NSCs with velocity dispersions $\gtrsim 40 \text{ km s}^{-1}$, since primordial binaries might not provide enough heat source via single-binary interactions that could support core collapse as in Lee (1987), Quinlan & Shapiro (1990). They found that during or after full core collapse, the stars will undergo runaway collisions that produce a black hole, which will then grow via tidal disruption of stars, a process that is expected to scale as $M_{\text{BH}}(t) \sim 10^6 M_{\odot} (\sigma/50 \text{ km s}^{-1})^{3/2} \sqrt{t/10^{10} \text{ yr}}$ (Stone et al. 2017). This can be considered further evidence to expect in galactic nuclei $M_{\text{BH}}/M_{\text{cluster}}$ efficiencies higher than the few percentage found in N-body simulations of globular-type stellar clusters.

Nevertheless, for velocity dispersions $\gtrsim 100 \text{ km s}^{-1}$, Miller and Davies (2012) argued that NSCs will typically have too long a relaxation time for its core to collapse within a Hubble time, a condition equivalent to the right side of the dashed green displayed in Fig. 1. However, they missed the possible new regime of global instability proposed here for $t_{\text{coll}} (\leq t_{\text{H}}) \leq t_{\text{relax}}$, for masses larger than when the dashed green line in Fig. 1 intersects the solid blue line and that strikingly coincides with the maximum mass scale with presence of NSCs in galactic nuclei. For $t_{\text{coll}} \leq t_{\text{relax}}$, relaxation processes will be unable to reverse global collapse before the onset of runaway collisions, which may lead to global collapse onto the formation of a MBH. Since the condition $t_{\text{coll}} \leq t_{\text{relax}}$ in Fig. 1 is computed for total NSCs quantities, is valid over the whole system and not restricted to the core, being also valid independent of different processes favoring or quenching core collapse analyzed by Miller and Davies (2012).

Therefore, Fig. 1 is supporting evidence that, in addition of NSCs being the most favorable places for stellar collisions, the most massive and denser NSCs that forms in the Universe might exist only temporarily, being in principle globally unstable to collapse to a MBH. This instability should be eventually triggered by runaway stellar collisions at some density limit, regardless if it is at the $\hat{\rho}_{\text{crit}}$ defined by Eq. 2 (for $t_{\text{coll}} \leq t_{\text{relax}}$) or another criterion that includes processes such as gas dissipation and others not taken into account. It is then possible to visualize the following transition in the properties of CMOs: for objects denser than some critical limit, which from the intersection defined by Eqs 2 and 4 at $t_{\text{H}} \sim 10^{10} \text{ yr}$, or from Eq 3 in order to fulfill the observed scaling relation for NSCs (Leigh et al. 2012), seems to be the case for $M_{\text{CMO}} \gtrsim 4 \times 10^8 M_{\odot}$, most of the CMO mass will be in the form of a MBH. On the opposite mass limit, the bulk of mass in the CMO will stay in the

stars of the NSC, even some cases with an undetectable MBH at its center, with black hole efficiencies $\epsilon_{\text{BH}} = M_{\text{BH}}/M_{\text{CMO}}$ probably in the range of star cluster simulations from 0.1% up to a few percent (Portegies Zwart & McMillan 2002; Freitag et al. 2006a,b; Sakurai et al. 2018; Reinoso et al 2018) until it approaches to a second critical mass ($M_{\text{CMO}} \sim 10^7 M_{\odot}$; according to Lee 1987; Quinlan & Shapiro 1990; Miller and Davies 2012; Stone et al 2017), where the black hole efficiency should have a drastic change, rapidly growing towards ϵ_{BH} close to 1.

3.1. Testing the Scenario for MBH Formation and Implications for Scaling Relations

The concordance of the proposed scenario for CMOs evolutionary paths, with the observed relative masses in MBHs and NSCs can be easily tested. Assuming that is the total mass in CMOs the mass reservoir for which competes MBHs and NSCs in galactic nucleus, $M_{\text{CMO}} = M_{\text{NSC}} + M_{\text{BH}}$, for a black hole formation efficiency (ϵ_{BH}) the central black hole mass is $M_{\text{BH}} = \epsilon_{\text{BH}} M_{\text{CMO}}$ and the mass of the surrounding nuclear cluster is then $M_{\text{NSC}} = (1 - \epsilon_{\text{BH}}) M_{\text{CMO}}$, both related to the efficiency as $\epsilon_{\text{BH}} = (1 + \frac{M_{\text{NSC}}}{M_{\text{BH}}})^{-1}$, which then it can be directly estimated by measuring the masses M_{NSC} and M_{BH} . Also, assuming that is total mass in central massive objects M_{CMO} the one that correlates with the total mass of the host spheroid ($M_{\text{CMO}} = \epsilon M_{\text{sph}}$, with $\epsilon \sim 0.1\%$; Magorrian et al. 1998), it is straightforward to realize that in both limiting cases (either only a MBH or a NSC), the observed (individual) relations are automatically fulfilled ($M_{\text{NSC}} \sim \epsilon M_{\text{sph}}$ for $\epsilon_{\text{BH}} \sim 0$ and $M_{\text{BH}} \sim \epsilon M_{\text{sph}}$ for $\epsilon_{\text{BH}} \sim 1$).

Fig 2 displays the efficiencies $\epsilon_{\text{BH}} = (1 + \frac{M_{\text{NSC}}}{M_{\text{BH}}})^{-1}$ plotted against the total mass in central massive objects ($M_{\text{CMO}} = M_{\text{NSC}} + M_{\text{BH}}$), both quantities computed using measured masses from a dataset collected (and homogenized) recently in the review by Neumayer et al. (2020), denoted by the black circles on the figure. The data in Fig 2 clearly displays three regimes: a) $\epsilon_{\text{BH}} \leq 0.15$ for $M_{\text{CMO}} \leq 3 \cdot 10^7 M_{\odot}$, b) $\epsilon_{\text{BH}} \geq 0.9$ for $M_{\text{CMO}} \geq 3 \cdot 10^8 M_{\odot}$ and c) a transition regime between $3 \cdot 10^7 M_{\odot} \leq M_{\text{CMO}} \leq 3 \cdot 10^8 M_{\odot}$ with rapidly growing ϵ_{BH} . Upper limits for the efficiencies ϵ_{BH} are denoted by lower triangles, while lower limits for ϵ_{BH} by upper triangles, displaying the same trend of the black circles, but with a larger scatter as expected for upper and lower limits. This trend is clear and suggestively in agreement with the proposed formation scenario for CMOs, with the transition regime limited on the expected boundaries defined by the ‘merger instability’ found in Fokker-Planck models of galactic nuclei ($\gtrsim 10^7 M_{\odot}$; Lee 1987; Quinlan & Shapiro 1990) and the upper limit given by the condition $t_{\text{coll}} \leq t_{\text{relax}}$ ($\gtrsim 10^8 M_{\odot}$, also in agreement with Eq 3 to fulfill the scaling

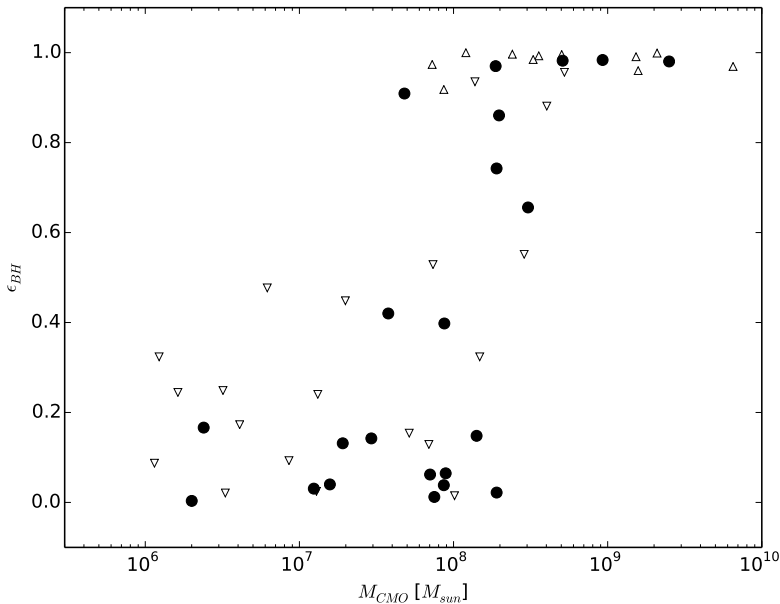


Fig. 2.— Observed black hole formation efficiency $\epsilon_{BH} = (1 + \frac{M_{NSC}}{M_{BH}})^{-1}$ as a function of the total mass in central massive objects $M_{CMO} = M_{NSC} + M_{BH}$, with both quantities computed using the MBHs and NSCs masses from the dataset by Neumayer et al. (2020), represented by black circles. The efficiency displayed in the figure has two dominant values for black hole efficiencies ($\epsilon_{BH} \leq 0.15$ at $M_{CMO} \leq 3 \cdot 10^7 M_{\odot}$ and $\epsilon_{BH} \geq 0.9$ for $M_{CMO} \geq 3 \cdot 10^8 M_{\odot}$) and a transition close to a step function of the mass. Upper limits for the efficiencies ϵ_{BH} are denoted by lower triangles, while lower limits for ϵ_{BH} by upper triangles, displaying the same trend of the black circles but with larger scatter at lower CMO masses.

relation for NSCs; Leigh et al. 2012). This can be contrasted, for example, with black hole efficiencies ϵ_{BH} that are randomly distributed between 0 and 1, which could be the case on a different formation scenario, where most (75%) of the measurements should be in the interval $\epsilon_{BH} = [0.15, 0.9]$ and where there is a total absence of black circles in regimes a) and b) of Fig 2. Moreover, a sharp transition is also seen around to $M_{CMO} \sim 10^8 M_{\odot}$, suggesting again that this is the limit for (collision-driven) global collapse, where most of the mass ends up into a single MBH and that naturally explains the lack of NSCs around MBHs for $M_{BH} \gtrsim 4 \cdot 10^8 M_{\odot}$ (Georgiev et al 2016).

The efficiency displayed in Fig 2, with two dominant values for BH efficiencies and a transition with a form close to a step function of the mass, could also explain the origin in the change of scaling in the M - σ relation from NSCs to MBHs, which has been taken as

support that MBHs and NSCs may not share a common origin (Leigh et al. 2012). The empirical evidence is that NSCs have a less steep scaling relation $M_{\text{NSC}} \propto \sigma^{2-3}$ (Leigh et al. 2012; Graham 2012), compared with the scaling for MBHs that have steeper slopes of $M_{\text{BH}} \propto \sigma^{4-5}$ (Ferrarese & Merritt 2000; Gebhardt et al. 2000). Assuming that CMOs have a single scaling relation originated in the galaxy formation process, for example, the scaling defined at the critical threshold given by Eq. 3 ($M_{\text{CMO}} \propto \sigma^{3.5}$), the step function efficiency ϵ_{BH} shown in Fig 2 bias the relation for the less massive MBHs, giving a steeper slope (> 3.5) for the MBH scaling relation and vice versa, $1 - \epsilon_{\text{BH}}$ bias the original relation for the more massive NSC giving a less steep slope (< 3.5). Therefore, this naturally reconcile an scenario of joint formation, with different M- σ scaling relation for MBHs and NSCs.

It is important to note, that alternative scenarios completely different from in-situ NSC formation have been also explored to explain NSC properties and the different scaling relations for NSCs and MBHs. For example, a widely studied scenario is that NSCs form via merging of orbitally migrated globular clusters (Tremaine et al. 1976; Capuzzo-Dolcetta 1993; Leigh et al. 2015). In those scenarios, tidal forces due to the gravity of a MBH can stop the NSC assembly by disrupting the orbitally in-falling clusters, leading also to a maximum mass scale for NSCs under the presence of MBHs (Antonini et al 2012, Arca Sedda et al 2015). Hybrid models of both migration of stellar clusters and in-situ formation in galactic nuclei has also been explored by means of semi-analytical/numerical models, which also explains the different M- σ relations for NSCs and SMBHs (Arca Sedda and Capuzzo-Dolcetta 2014, Antonini et al 2015). The biggest advantage of the scenario outlined in this paper is its simplicity, giving a clear cause for the sharp transition in Fig. 2 for clusters becoming globally unstable against collisions for $t_{\text{coll}} \leq t_{\text{relax}}$, at the correct mass-scale for clusters with ages comparable to the current age of the universe (Fig. 1), that in addition naturally explains different M- σ scaling relation for MBHs and NSCs, compared with more complex (and multifactorial) explanations in these alternative models.

4. Discussion

We explored an scenario for MBH formation driven by stellar collisions in galactic nuclei, proposing a new formation regime of global instability in NSCs triggered by runaway stellar collisions, for central massive objects that have average relaxation times longer that their collision times. For systems with ages comparable to the Hubble time, this condition is fulfilled for objects more massive than $\sim 4 \times 10^8 M_{\odot}$, being in principle subject to be globally unstable against stellar collisions, where most of its mass may collapse towards the formation of a MBH, being effectively the fate of failed stellar cluster. Contrarily, this will only be the

case at the core of less dense central massive objects leading to the formation of MBHs with much lower efficiencies ϵ_{BH} . We showed that the proposed scenario successfully explains the relative trends observed in the masses, efficiencies and scaling relations between MBHs and NSCs.

The proposed scenario links naturally to the fact that the existence MBHs in galaxies is intimately related with their spheroidal/triaxial component (Ferrarese & Merritt 2000; Gebhardt et al. 2000), that is supported by random motions and where collisions are much more frequent compared to the disk component of galaxies (for a given characteristic velocity), since disks are systems that are rotationally supported and their ordered motions prevents collisions. In addition, this collision driven global instability in extreme stellar systems sets internally the upper mass limit of NSCs around $\sim 10^8 M_{\odot}$, something needed because at galactic scales the study of gravitational instabilities do not set externally an upper limit for the stellar cluster masses in galactic nuclei, since the size of the whole system is the largest unstable wavelength (Jeans 1902). Only when rotation becomes relevant (i.e. in the galactic disk), this sets a maximum mass scale for a gaseous collapsing cloud, ranging from $M_{\text{cloud}}^{\text{max}} \sim 10^6 M_{\odot}$ for MW type disks, upto the order of $\sim 10^8 M_{\odot}$ for ULIRGs nuclear disks (Escala & Larson 2008). Those massive clouds in ULIRGs are expected to migrate and runaway merge in galactic nuclei (Elmegreen et al. 2008), again lacking of an externally defined upper limit.

A relevant issue not studied in extent in this paper is the role of gas in the formation and evolution of NSCs, particularly, in the enhancement of stellar collisions. Although the details in the exact evolution of the gaseous (and stellar) material funneled into galactic nuclei are still unclear under realistic conditions, some idealized analytical estimations can be made. For example, Davies, Miller & Bellovary (2011) concluded that a typical NSC at high z (mass $\sim 10^6 M_{\odot}$ and size ~ 1 pc) can be contracted on dynamical timescales due to gas inflow with a mass up to ten times heavier than the pre-existing stellar mass (according to cosmological simulations; Bellovary et al. 2011), then reach a central density high enough for triggering a phase of runaway collisions that could form a MBH seed of $10^5 M_{\odot}$ or larger. Moreover, these high central densities (and thus runaway collisions) can be enhanced by the gaseous dynamical friction, that can be an efficient process to lead the migration of additional stellar compact remnants to galactic nuclei (Boco et al 2020).

However, all these gas dynamical processes relevant for high z (proto-)clusters act on local dynamical timescales, short compared to the current age of the universe, therefore, is relevant to see how the proposed regime of collision-driven global instability can work under such shorter timescales. Fig 3 display collision and relaxation timescales that are equals to cluster ages (t_{H}) of 10^{10} yr in blue, 10^8 yr (green) and 10^6 yr (purple), which illustrates

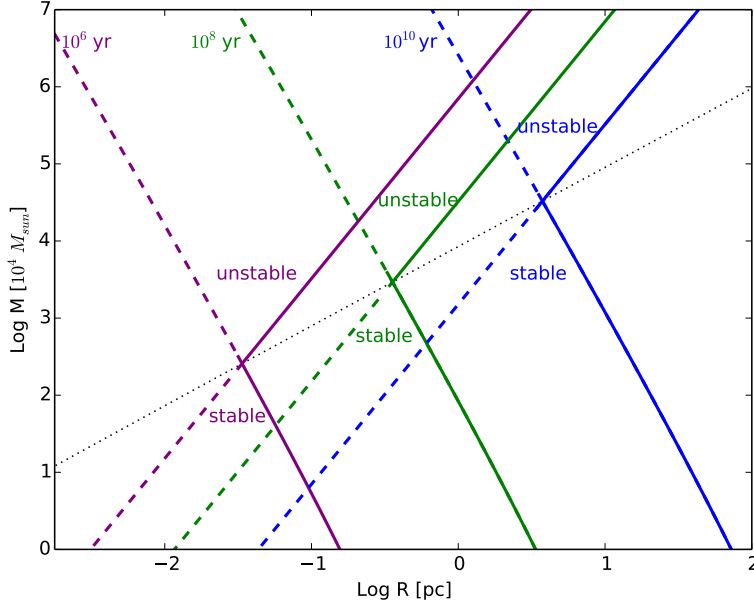


Fig. 3.— Collision and relaxation timescales in the mass versus radius diagram, for different cluster ages t_H : 10^{10} yr (blue), 10^8 yr (green) and 10^6 yr (purple). For each color with a different t_H , clusters in the left side of the solid curves fulfill the condition $t_{\text{coll}} \leq t_H$ or $t_{\text{relax}} \leq t_H$, with the intersection of solid curves dividing the stable ($t_{\text{relax}} \leq t_{\text{coll}}$) and the unstable ($t_{\text{coll}} \leq t_{\text{relax}}$) regions. The dotted black line denotes the condition $t_{\text{relax}} = t_{\text{coll}}$.

that one order of magnitude of contraction in effective radius, for example, due to the gaseous inflows expected at high z (Davies, Miller & Bellovary 2011), can effectively reduce in almost four orders of magnitude the time required for collisions to become relevant (from t_{coll} being comparable to the Hubble time down to $\sim 10^6$ yr). The dotted black line denotes the condition $t_{\text{relax}} = t_{\text{coll}}$, equivalent to $R/R_\odot = [\ln(M/M_\odot)/7.5]^{-1/2} M/M_\odot$, valid regardless of the cluster age.

The left side of solid lines denotes the region where 2-body relaxation or collisions can be relevant (i.e shorter than t_H), thus subject to be globally unstable to stellar collisions for $t_{\text{coll}} (\leq t_H) \leq t_{\text{relax}}$ and globally stable for $t_{\text{relax}} \leq t_{\text{coll}}$. If the discussed gas dynamical processes are able to populate clusters in the region denoted as ‘unstable’ in green and purple on Fig 3, they will be subject to runaway stellar collisions over the whole system on shorter timescales, possibly leading to the formation of ‘naked’ MBHs (i.e. without a surrounding cluster) with lower masses than currently observed in NSCs: $M_{\text{BH}} \gtrsim 3 \times 10^7 M_\odot$ for $t_H \sim 10^8$ yr

(green) and $M_{\text{BH}} \gtrsim 3 \times 10^6 M_{\odot}$ for $t_{\text{H}} \sim 10^6 \text{yr}$ (purple). In the region below that threshold (intersection of solid lines), relaxation processes will operate and the cluster will expand before the onset of runaway collisions is triggered over the whole system, being such collisions restricted to the unstable core and thus a central MBH is possibly formed that coexists with a surrounding NSC.

Most probably the extremely dense, purely gas-free NSC discussed in this paper rarely exists in the early Universe and most often, an unstable NSC will collapse as a whole during its formation, before evaporating its gaseous envelope, as might be suggested by the multiple stellar populations seen in the surviving NSCs (Nishiyama & Schodel 2012). On the other hand, if the formation of this surviving NSCs was occurring at high redshift, these would likely be observable with James Webb Space Telescope (JWST). Since the progenitors of globular clusters are already expected to be detected at high- z ($3 \lesssim z \lesssim 8$; Renzini 2017), these most massive progenitors of NSCs should be more likely to be detected, as the number of clusters that could be detected scales linearly with their mass (Renzini 2017).

Certainly, more realistic simulations (with and without gaseous components) are needed to set the open issues, but the absence of NSCs in the collision-dominated regime, with the sharp transition seen at the boundaries of the unstable region of Fig 1, suggests that the fate of the unstable ones is unavoidably collapsing onto a MBH. Therefore, besides all these uncertainties, the results in this work can be taken as supporting evidence that the collapse leading to MBH formation is most probably triggered by runaway collisions, than by suppressing fragmentation on smaller scales or alternatively, by the runaway growth of a preferred IMBH on cosmological timescales. Also, this collision-driven BH formation is a process that could happen even in the the earliest epochs of the Universe (Korol et al. 2019), without imposing strict constraints on cosmological timescales.

Because it is hard to constrain enough MBH formation thru direct observations of such objects by traditional electromagnetic detections, in addition of having more complex and realistic simulations, definite answers will probably come from direct observations of the final collapse by gravitational-wave observatories such as LISA (Amaro-Seoane et al. 2013). In the complex collision-driven collapse scenario described in this letter, it is hard that the final collapsing VMS will be close to spherically or axially symmetric, therefore, it is expected to be at least bar-shaped and most probably, even more irregular and a gravitational wave signal it is expected from galactic centers at the moment of MBH formation (Rees 1984), that will be detectable in the LISA band out to high redshift (Sun et al. 2017).

REFERENCES

- Amaro-Seoane, P., et al. 2013, arXiv:1305.5720
- Antonini F., Capuzzo-Dolcetta R., Mastrobuono-Battisti A., Merritt D., 2012, ApJ, 750, 111
- Antonini F., et al. 2015, ApJ, 812, 72
- Arca-Sedda M., & Capuzzo-Dolcetta R., 2014, MNRAS 444, 3738-3755
- Arca-Sedda M., Capuzzo-Dolcetta R., Antonini F., Seth A., 2015, ApJ, 806, 220
- Agarwal B, Davis AJ, Khochfar S, Natarajan P, Dunlop JS. 2013. MNRAS 432: 3438-3444
- Banerjee, S., & Kroupa, P. 2017, A&A 597, A28
- Balcells M., Graham A. W., & Peletier R. F., 2007, ApJ, 665, 1104
- Barause, E., et al. 2015, Journal of Physics Conference Series 610(1)
- Barnes, J. E. 2002, MNRAS, 333, 481
- Bate, M. R., et al. 2003, MNRAS, 339, 577-599
- Baumgardt, H., Amaro-Seoane, P., Schodel, R. 2018, A&A 609, A28
- Becerra F, et al. 2015, MNRAS, 446, 2380-2393
- Bellovary, J., Volonteri, M., Governato, F., et al. 2011, ApJ, 742, 13
- Binney, J., & Tremaine, S. 2008, Galactic Dynamics, Princeton Univ. Press
- Boco, L., et al. 2020, ApJ, 891, 94
- Boker T., et al. 2004, AJ, 127, 105
- Bromm, V., & Loeb, A. 2003, ApJ, 596, 34
- Cappellari M. et al., 2006, MNRAS, 366, 1126
- Capuzzo-Dolcetta R., 1993, ApJ, 415, 616
- Cote, P., et al., 2006, ApJS, 165, 57
- Davies, M.B., Miller, M.C., & Bellovary, J.M. 2011, ApJ, 740, L42
- Devecchi B, Volonteri M. 2009. ApJ 694:302-313

- Dubois, Y., Volonteri, M., Silk, J., et al. 2015, MNRAS, 452, 1502
- Elmegreen, B. G., Bournaud, F., & Elmegreen, D. M. 2008, ApJ, 684, 829-834
- Escala, A., 2006, ApJ, 648, L13
- Escala, A., 2007, ApJ, 671, 1264
- Escala, A. & Larson, R. B. 2008, Apj, 685, L31
- Escala, A., 2011, ApJ, 735, 56
- Ferrarese, F. , & Merritt, D. 2000, ApJ, 539, L9-L12
- Ferrarese, L., et al., 2006, ApJ, 644, L2
- Freitag, M., Gurkan, M. A., & Rasio, F. A. 2006, MNRAS, 368, 141
- Freitag, M., Rasio, F. A., & Baumgardt, H. 2006, MNRAS, 368, 121
- Gebhardt, K. et al. 2000, ApJ, 539, L13-L16
- Georgiev, I. Y. et al 2016, MNRAS, 457, 2122-2138
- Ghez et al. 2008, ApJ, 689, 1044
- Gieles, M., Moeckel N. and Clarke, C.J. 2012, MNRAS, 426, L11
- Gillessen et al. 2009, ApJL, 707, L114
- Gnedin, O. Y. 2001, Class & Quant. Grav., 18, 3983
- Goswami, S., Umbreit, S., Bierbaum, M., & Rasio, F. A. 2012, ApJ, 752, 43-55
- Graham, A. W. 2012, MNRAS, 422, 1586-1591
- Gultekin, K., et al, 2009, ApJ, 698, 198
- Gurkan, M. A., Freitag, M., & Rasio, F. A. 2004, ApJ, 604, 632-652
- Henon, M. 1965, Ann. Astrophys., 28, 62.
- Hopkins, P. F. & Quataert, E. 2010, MNRAS, 407, 1529
- Inayoshi, K., & Haiman, Z. 2014 MNRAS, 445, 1549-155
- Inayoshi, K., et al. 2020 Annu. Rev. Astron. Astrophys., 204, 9-0, 4455

- Jeans, J.H. 1902, *Phil. Trans. Roy. Soc. London, ser. A*, 199, 1-53
- Korol, V., Mandel, I., Miller, M.C. et al. 2019 arXiv:1911.03483
- Landau, L. D., Lifshitz, E. M. 1980, *Statistical Physics, Vol. 5*, Butterworth-Heinemann
- Latif, M.A., & Schleicher, D.R.G. 2015. *A&A* 578:A118
- Lee, H. M. 1987, *ApJ*, 319, 801
- Leigh, N., Boker, T., Knigge, C. 2012, *MNRAS*, 424, 2130
- Leigh, N. et al 2014, *MNRAS*, 444, 29
- Leigh, N. et al 2015, *MNRAS*, 451, 859
- Lodato, G., & Natarajan, P. 2006, *MNRAS*, 371, 1813L
- Madau, P., & Rees, M. J. 2001, *ApJ*, 551, L27
- Magorrian, J., et al. 1998, *ApJ*, 115, 2285-2305.
- Mayer, L., et al 2010, *Nature* 466, 1082-1084
- Miller, M.C., & Davies, M.B. 2012, *ApJ*, 755, 81-88
- Nishiyama, S., & Schodel, R. 2012, *A&A*, 549: A57
- Oppenheimer, J. R.; Volkoff, G. M. 1939. *Physical Review*, 55, 374-381
- Padoan, P. et al. 2016, *ApJ*, 826, 140
- Pamanarev, T., et al. 2019, *MNRAS*, 484, 3279
- Portegies Zwart, S. F., et al. 1999, *A&A*, 348, 117
- Portegies Zwart, S. F., & McMillan, S. L. W. 2002, *ApJ*, 576, 899
- Prieto, J., & Escala, A. 2016, *MNRAS*, 460, 4018-4037
- Prieto, J, Escala, A., Volonteri, M., & Dubois, Y. 2017, *ApJ*, 836, 216
- Prieto, J., Escala, A, & Privon 2020 submitted
- Quinlan, G. D., & Shapiro, S. L. 1990, *ApJ*, 356, 483
- Rees, M. J., & Ostriker, J. P. 1977, *MNRAS*, 179, 541

- Rees, M. J. 1984, *ARA&A*, 22, 471
- Regan, M. W., & Teuben, P. J. 2004, *ApJ*, 600, 595-612
- Regan, J.A., Downes, T.P., 2018. *MNRAS* 475:4636-4647
- Reinoso, B., et al 2018, *A&A*, 614, A14
- Renzini, A., 2017, *MNRAS*, 469, L67
- Ricarte, A., Natarajan, P., 2018. *MNRAS* 481:3278-3292
- Sakurai, Y., Yoshida, N., Fujii, M. S., & Hirano, S. 2018, *ApJ*, 855, 17
- Salpeter, E. 1964, *ApJ*, 140, 796
- Sanders, R. H. 1970, *ApJ*, 162, 791
- Sarazin, C. L., & White, R. E. 1987, *ApJ*, 320, 32
- Schleicher, D. R. G. et al. 2013, *A&A*, 558, A59
- Shang C., Bryan G.L., & Haiman Z. 2010, *MNRAS*, 402, 1249-1262
- Shapiro, S. L. & Teukolsky, S. A. 1985, *ApJ*, 292, L41
- Shapiro, S. L. 2004, in *Carnegie Observatories Astrophysics Series, Vol. 1: Coevolution of Black Holes and Galaxies*, ed. L. C. Ho (Cambridge: Cambridge Univ. Press), 103
- Shlosman, I., Begelman, M. C., & Frank, J. 1990, *Nature*, 345, 679
- Shu, F. H., 1991, *The Physics of Astrophysics, Vol. 2*, University Science Books
- Spergel D. N. et al., 2003, *ApJS*, 148, 175
- Spitzer, L. J. 1969, *ApJ*, 158, L139
- Stone, N.C., Kupper, A.H.W., Ostriker, J.P. 2017, *MNRAS*, 467:4180-4199
- Suazo, M., Prieto, J., Escala, A., Schleicher, D. R. G. 2019, *ApJ*, 885, 127
- Sun, L. et al. 2017, *Phys.Rev.D*, 96, 4, 043006
- The Event Horizon Telescope Collaboration, 2019, *ApJL*, 875, L1-L6
- Tolman, R. C. 1934, *PNAS*, 20, 169-176

- Toomre, A. 1964, ApJ, 139, 1217
- Tremaine S. D., 1976, ApJ, 203, 345
- Vishniac, E. T. 1978, ApJ, 223, 986
- Volonteri, M. et al. 2003. ApJ, 582, 559-573
- Volonteri, M., & Rees, M. J. 2006, ApJ, 650, 669-678
- Volonteri, M., & Begelman, M.C. 2010, 409, 1022-1032
- Volonteri, M. 2010, A&A Review, 18, 279-315
- Walcher C. J. et al.,2006, ApJ, 649, 692
- Zel'dovich, Ya. 1964, Soviet Phys., 9, 195
- Zel'dovich, Ya. B., & Podurets, M. A. 1965, Astron. Zh., 42, 963